Available online at www.sciencedirect.com
SCIENCE DIRECT®
Journal of Sound and Vibration 287 (2005) 591–610
JOURNAL OF SOUND AND VIBRATION
www.elsevier.com/locate/jsvi

Coupled bending and torsional vibration of a beam with in-span and tip attachments

Hakan Gökdağ*, Osman Kopmaz

Department of Mechanical Engineering, College of Engineering and Architecture, Uludağ University, Görükle, Bursa 16059, Turkey

Received 5 January 2004; received in revised form 12 November 2004; accepted 18 November 2004
Available online 12 February 2005

Abstract

In this paper, the coupled flexural–torsional free and forced vibrations of a beam with tip and/or in-span attachments are studied. First, a mathematical model is established, which consists of a beam with several tip attachments, i.e, a tip mass of non-negligible dimensions, a linear spring grounding the tip mass, and a torsional spring connected at the end of the beam. The modal functions of this model and the orthogonality condition among them are derived. For the purpose of verification the properties of the tip attachments are changed, and the numerical results obtained are compared with those given in the relevant literature. Effects of tip mass and distributed mass in-span on natural frequencies and modes are investigated for two cantilever beams with different cross sections. An application of the orthogonality condition in the case of a beam with tip mass is also presented for a forced vibration example.

1. Introduction

The dynamic behavior of beams with attachments has been investigated by many authors owing to increased applications for such structures. In this context, Abromovich and Hamburger [1] studied how the frequencies of a system that may be considered as a flexible robot arm vary with respect to some characteristic properties of beam and attachments. The system in that work

*Corresponding author. Fax: +90 224 442 80 21.
E-mail addresses: hakangkd@uludag.edu.tr (H. Gökdağ), okopmaz@uludag.edu.tr (O. Kopmaz).

0022-460X/$ - see front matter © 2004 Elsevier Ltd. All rights reserved.
doi:10.1016/j.jsv.2004.11.019

Nomenclature

$\hat{\mathbf{A}}$	eigenvalues matrix
$\bar{B}$	the domain occupied by the tip mass
$\hat{\mathbf{C}}$	column matrix of modal amplitude coefficients
c	shear center offset
$EI_z, GJ, E\Gamma$	bending, torsional and warping rigidities of beam, respectively
F_a, F_b, F_c, F_d	four right-handed coordinate frames with the unit vectors $\mathbf{a}_i, \mathbf{b}_i, \mathbf{c}_i, \mathbf{d}_i$, respectively (see Fig. 2)
$\bar{G}$	gravitational center of the tip mass
I_c	mass moment of inertia of the cross section per unit length with respect to the centroidal axis
I_s	mass moment of inertia of the cross section per unit length with respect to the shear center axis ($I_s = I_c + mc^2$)
I_z	the second moment of area about z-axis
$I_{\bar{x}\bar{x}}$, $I_{\bar{z}\bar{z}}$, $I_{\bar{x}\bar{z}}$	components of the inertia tensor about the center of gravity of the tip mass
$\hat{I}_{\bar{z}\bar{z}}$, $\hat{I}_{\bar{x}\bar{x}}$, $\hat{I}_{\bar{x}\bar{z}}$	components of the inertia tensor about the end of the beam (point S in Fig. 1)
k_L	stiffness of the linear spring attached to the tip mass
k_T	stiffness of the torsional spring attached to the end of the beam
$\mathbf{K}_T$	stiffness matrix
L	beam length
$\mathbf{M}_T$	mass matrix
M	tip mass amount
m	beam mass per unit length
O	the root point of the beam (the origin of the frame F_a)
P	location point of a differential tip mass element
$\mathbf{Q}$	column matrix of generalized forces
$\widehat{\mathbf{q}}$	generalized coordinates in the case of forced vibration
$\hat{\mathbf{q}}$	generalized coordinates in the case of free vibration
$\mathbf{r}_P$	displacement vector of a differential tip mass element located at point P
S	the end point of the elastic axis of beam
T	overall kinetic energy of the beam with attachments
t	time parameter
U	overall potential energy of the beam with attachments
$V(x)$	modal amplitude functions related to bending deformation
$\mathbf{V}$	column matrix including modal amplitude functions $V(x)$
$w(x,t)$	deflection function of beam
w_L	deflection at the beam end with tip mass ($w_L = w(L,t)$)
x	spatial coordinate parameter
Y	attachment point of the linear spring to the tip mass
α	slope angle at the end with tip mass of beam ($\alpha = w_x(L,t)$)
β	torsion angle at the end with tip mass of beam ($\beta = \psi(L,t)$)
$\psi(x,t)$	torsional deformation function of beam
ψ_L	torsional deformation at the end with tip mass of beam ($\psi_L = \psi(L,t)$)
$\Delta\mathbf{Y}$	displacement vector of the point Y (Fig. 1) along the y-axis
ω	frequency parameter of the system without distributed mass
ϖ	frequency parameter of the system including distributed mass
$\boldsymbol{\theta}$	column matrix including modal amplitude functions $\theta(x)$
$\theta(x)$	modal amplitude functions related to torsional deformation
"$\cdot$"	derivative with respect to time t
"$'$"	derivative with respect to spatial coordinate x

consists of a cantilever Timoshenko beam with uniform cross section, translational and rotational springs attached in-span, and a tip mass of considerable dimensions. A similar system was examined by Gürgöze [2]. The system in Ref. [2] is a cantilever beam with a concentrated tip mass

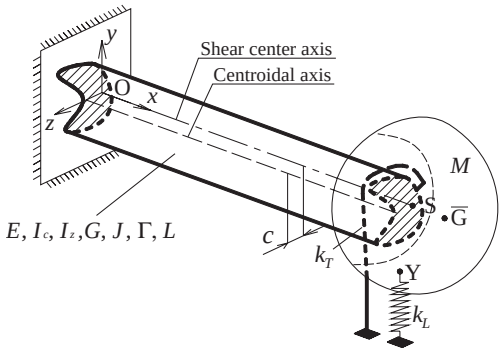

Fig. 1. The system consisting of an Euler–Bernoulli beam with tip mass and springs.

to which another discrete spring–mass system is attached. Gürgöze derived the frequency equation of the system by using the assumed modes method in conjunction with the Lagrange multipliers method, and also obtained the frequency equation of some subsystems by limiting procedure. In Refs. [3,4], attachment effects are considered from different points of view by means of various solution procedures. In a recent paper [5], Oguamanam investigated a cantilever beam with a rigid tip mass, whose center of gravity is not coincident with the attachment point. Due to the existence of an out-of-plane payload, the beam studied in Ref. [5] experiences torsional deformation along with a planar elastic bending deformation. The effects of some attachment parameters such as the amount and the moment of inertia of the tip mass on the fundamental frequency of the system are examined via corresponding non-dimensional terms. In the papers cited so far, the models are based on the assumption that the beam under study has double symmetry axes; hence, the centroidal axis and the shear center axis of the beam are coincident. However, beams for which these two axes are different are used in certain engineering structures. For instance, an airplane wing with engines requires a different beam model from those considered in the above works. Similarly, a flexible robot arm of monosymmetric cross section needs to be modeled as a beam undergoing coupled bending and torsional deformations if it does not vibrate in the plane of symmetry. For this reason, some representative examples of the works which deal with the beams having monosymmetric cross sections will also be mentioned below.

Beams with a single axis of symmetry perform coupled flexural–torsional vibrations due to the separation of centroidal and shear center axis. For such a beam with uniform cross section, the governing differential equations appear to be a pair of coupled equations with constant coefficients. Timoshenko et al. [6] presented these equations for a beam having simply supported ends. Ignoring the warping effect, Dokumaci [7] determined the coupled free vibration frequencies of a cantilever beam. Later, his work was extended by Bishop et al. [8] by including the warping effect. The latter authors demonstrated that neglecting warping term in the equations of motion could cause misleading results. Since the torsional stiffness of a beam with open cross section is much less than that of a beam with solid cross section of the same size, ignoring the warping term causes a decrease in natural frequencies as indicated in Ref. [8]. Bercin and Tanaka [9] also studied the coupled flexural and torsional vibrations of beams including warping, shear deformation and rotatory inertia effects. The numerical results presented in Ref. [9] support the claim that these

section effects become more significant as the thickness of the beam and the modal index increase. In Ref. [10], Banerjee derived explicit analytical expressions giving the natural frequencies and mode shapes of a cantilever beam performing coupled bending and torsional vibrations. In this work, however, the warping effect is excluded. A method for the analysis of forced coupled flexural–torsional vibrations of distributed parameter beams was presented by Adam in Ref. [11]. Eslimy-Isfahany and Banerjee [12] interpreted the mode shapes and the dynamic response of bending–torsion coupled beams by using the concept of generalized mass. In the last two papers, the forced vibrations of such beams are treated, as well. Hashemi and Richard [13] developed a dynamic finite element formulation for the free vibration analysis of such beams subject to an axial load. Taking the warping effect into account, Jun et al. [14] carried out the free vibration analysis of an axially loaded beam with uniform open cross section by means of dynamic transfer matrix method.

In the works concerned with bending–torsion coupled beams having a single symmetry axis, it is observed that attachment effects are omitted. Therefore, the present paper primarily aims at developing a general method for the analysis of free and forced vibrations of a monosymmetric cross section beam with attachments at the tip and/or in-span. To this end, the kinetic and potential energy expressions of the system are derived by using the Euler–Bernoulli beam theory, including the warping of beam. Equations of motion and the associated boundary conditions are obtained by applying Hamilton's principle. Then, the modal amplitude functions and the characteristic determinant giving the natural frequencies of system are found by employing the conventional method of separation of variables. Furthermore, the orthogonality relationship among modal functions is derived. Then, these modal amplitude functions are used as comparison functions in the Galerkin's discretization procedure in order to analyze the dynamic behavior of the beam carrying a distributed mass in-span. The effects of attachments on natural frequencies and modal shapes are examined by means of computer codes written in MATLAB environment, and the results are presented in tables and graphics.

2. Boundary value problem formulation

The system to be studied is depicted in Fig. 1 in its undeformed state. The basic element of the system is the beam that is of length L and has a monosymmetric uniform open cross section. When the beam does not deflect, the x-axis represents the shear center axis of the beam. A rigid tip mass M of finite dimensions is attached to the beam at its right end, and is grounded via a linear spring of stiffness k_L at point Y. The center of gravitation $\bar{G}$ of the tip mass need not be coincident with that of the beam cross section at the connection plane. Furthermore, the right end of the beam is supported by a torsional spring of stiffness k_T, while the left end ($x = 0$) may be clamped or simply supported.

During free vibration, a possible configuration of the system is as shown in Fig. 2. The deformation of a differential beam element located at a distance x from the left end is defined by lateral displacement $w(x, t)$ in the y-direction and rotation $\psi(x, t)$ about the x-axis. Similar to Ref. [5], four orthogonal right-handed coordinate frames F_a, F_b, F_c, F_d are used in order to describe the position vector $\mathbf{r}_P$ of a differential element $\mathrm{d}M$ at a point P of the tip mass. In Fig. 2, frame F_a with unit vectors $\mathbf{a}_i$ ($i = 1, 2, 3$) is a Newtonian (or inertial) frame which has an origin

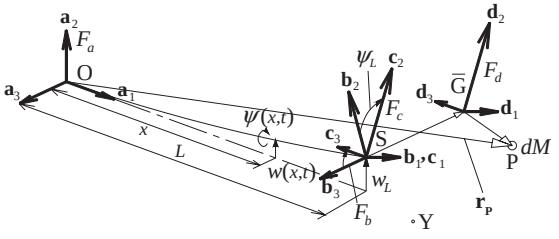

Fig. 2. Configuration of the system at a time t.

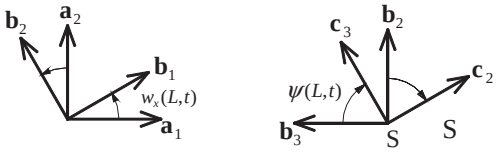

Fig. 3. Three orthogonal right-handed reference frames.

fixed at point O. The origins of the frames F_b and F_c are coincident, and these origins are fixed to point S undergoing a displacement denoted by w_L ($w_L = w(L,t)$). Relative displacement between these frames is such that the rotation of the frame F_c about $\mathbf{c}_1$ unit vector is equal to the torsion angle $\psi_L = \psi(L,t)$ at the right end of the beam. The orientations of these frames at a time during free vibration are also shown in Fig. 3. The fourth reference frame, F_d, is attached to the center of the tip mass. The unit vectors of the aforementioned frames are arranged in such a manner that $\mathbf{a}_3$ parallel to $\mathbf{b}_3$, $\mathbf{b}_1$ and $\mathbf{c}_1$ coincident, all unit vectors of frame F_c are parallel to corresponding ones of the frame F_d; $\mathbf{c}_i \equiv \mathbf{d}_i$ $(i = 1,2,3)$. The reference frames in which the coordinates of some important points are measured are given in Table 1, and illustrated in Fig. 3. A list of symbols used in the present study is given in the Nomenclature as well.

Kinetic and potential energy terms of the system in free vibration are derived as follows:

$$T = \frac{1}{2}\left(\int_0^L m(\dot{w} + c\dot{\psi})^2\,\mathrm{d}x + \int_0^L I_c\dot{\psi}^2\,\mathrm{d}x + \int_{\bar{B}} (\dot{\mathbf{r}}_P)^2\,\mathrm{d}M\right) \tag{1}$$

$$U = \frac{1}{2}\left(\int_0^L EI_z(w_{xx}^2)\,\mathrm{d}x + \int_0^L GJ(\psi_x^2)\,\mathrm{d}x + \int_0^L E\Gamma(\psi_{xx}^2)\,\mathrm{d}x + k_L(\Delta\mathbf{Y})^2 + k_B(\psi_L)^2\right) \tag{2}$$

where c is the shear center offset, the overhead dot denotes partial derivatives with respect to time t while subscript x represents partial derivatives with respect to spatial variable x. This notation will be used throughout the paper. I_z shows the second moment of area about the z-axis, I_c stands for the mass moment of inertia of the cross section per unit length with respect to the centroidal axis, m represents mass per unit length of the beam, EI_z, GJ and $E\Gamma$ are bending, torsional and warping rigidities, respectively. The last integration in Eq. (1) is to be performed over the domain $\bar{B}$ covered by the tip mass. Assuming that the deformation of the linear spring of stiffness k_L is

Table 1
Points in Fig. 1 with the relevant reference frames

Point	Related reference frame
$O(0,0,0)$	F_a
$S(L, w_L, 0)$	F_a
$\tilde{G}(p, q, s)$	F_c
$P(\bar{p}, \bar{q}, s)$	F_d
$Y(\bar{x}, \bar{y}, \bar{z})$	F_c

mainly due to the displacement of the point Y along y-axis, $\Delta\mathbf{Y}$ in Eq. (2) represents the component in the y-direction of the displacement vector of this point (other components are neglected). Using Eqs. (1) and (2) to construct Hamilton's integral

$$\delta \int_{t_1}^{t_2} (T - U)\,\mathrm{d}t = 0 \tag{3}$$

and implementing conventional principles of the variational calculus lead to the following equations of motion

$$EI_z w_{xxxx} + m(\ddot{w} + c\ddot{\psi}) = 0, \tag{4a}$$

$$E\Gamma\psi_{xxxx} - GJ\psi_{xx} + mc(\ddot{w} + c\ddot{\psi}) + I_c\ddot{\psi} = 0, \tag{4b}$$

along with the following boundary conditions:

$(x = 0)$:

$$\text{Free: } EI_z w_{xx} = 0,\ EI_z w_{xxx} = 0,\ GJ\psi_x - E\Gamma\psi_{xxx} = 0,\ E\Gamma\psi_{xx} = 0. \tag{5a}$$

$$\text{Clamped: } w = 0,\ w_x = 0,\ \psi = 0,\ \psi_x = 0. \tag{5b}$$

$$\text{Simply supported: } EI_z w_{xx} = 0,\ w = 0,\ E\Gamma\psi_{xx} = 0,\ \psi = 0. \tag{5c}$$

$(x = L)$:

$$EI_z w_{xxx} - M(\ddot{w} + \ddot{w}_x p + \ddot{\psi} s) - k_L(w_x\bar{x} + \psi\bar{z} + w) = 0, \tag{5d}$$

$$E\Gamma\psi_{xxx} - GJ\psi_x - \hat{I}_{\bar{x}\bar{x}}\ddot{\psi} - Ms\ddot{w} - \ddot{w}_x\hat{I}_{\bar{x}\bar{z}} - k_L(w_x\bar{z}\bar{x} + \psi\bar{z}^2 + w\bar{z}) - k_B\psi = 0, \tag{5e}$$

$$EI_z w_{xx} + \ddot{w}_x\hat{I}_{\bar{z}\bar{z}} + \ddot{w}pM + \ddot{\psi}\hat{I}_{\bar{x}\bar{z}} + k_L(w_x\bar{x}^2 + \psi\bar{x}\bar{z} + w\bar{x}) = 0, \tag{5f}$$

$$E\Gamma\psi_{xx} = 0 \quad \text{or} \quad \psi_x = 0, \tag{5g}$$

where

$$\hat{I}_{\bar{z}\bar{z}} = I_{\bar{z}\bar{z}} + M(q^2 + p^2), \quad \hat{I}_{\bar{x}\bar{x}} = I_{\bar{x}\bar{x}} + M(s^2 + q^2), \quad \hat{I}_{\bar{x}\bar{z}} = I_{\bar{x}\bar{z}} + Mps,$$

$$I_{\bar{x}\bar{z}} = \int_{\bar{B}} \bar{p}\bar{s}\,\mathrm{d}M, \quad I_{\bar{z}\bar{z}} = \int_{\bar{B}} (\bar{q}^2 + \bar{p}^2)\,\mathrm{d}M, \quad I_{\bar{x}\bar{x}} = \int_{\bar{B}} (\bar{q}^2 + \bar{s}^2)\,\mathrm{d}M. \tag{6}$$

$I_{\bar{x}\bar{x}}$, $I_{\bar{z}\bar{z}}$ and $I_{\bar{x}\bar{z}}$ in Eq. (6) are components of the inertia tensor about the center of gravity of the tip mass, while $\hat{I}_{\bar{z}\bar{z}}$, $\hat{I}_{\bar{x}\bar{x}}$ and $\hat{I}_{\bar{x}\bar{z}}$ represent the components of the inertia tensor about point S in Fig. 2 (for details, see Appendix A). Theoretically, the first of Eq. (5g) means that the tip mass can be mounted to the beam in the manner that warping occurs, whilst the second of Eq. (5g) represents the case in which no warping is possible. In the present study, the first of Eq. (5g) will be taken into account unless the tip mass exists.

Different from Ref. [5], where coupling between bending and torsion occurs only via the boundary conditions at the beam end with tip mass, there is also coupling in the equations of motion for the system studied in the present work.

Assuming harmonic motion with frequency ω, the solutions of the equations of motion are of the following form

$$w(x,t) = V(x)\mathrm{e}^{\mathrm{j}\omega t}, \quad \psi(x,t) = \theta(x)\mathrm{e}^{\mathrm{j}\omega t}, \quad \mathrm{j} = \sqrt{-1}, \tag{7}$$

where $V(x)$ and $\theta(x)$ are amplitude functions of $w(x,t)$ and $\psi(x,t)$, respectively. Substituting Eq. (7) into Eqs. (4) and (5) yields

$$EI_z V'''' - \omega^2 m(V + c\theta) = 0, \tag{8a}$$

$$E\Gamma\theta'''' - GJ\theta'' - \omega^2 mc(V + c\theta) - \omega^2 I_c\theta = 0, \tag{8b}$$

$$EI_z V''(0) = 0, \quad EI_z V'''(0) = 0, \quad GJ\theta'(0) - E\Gamma\theta'''(0) = 0, \quad E\Gamma\theta''(0) = 0, \tag{9a}$$

$$V(0) = 0, \quad V'(0) = 0, \quad \theta(0) = 0, \quad \theta'(0) = 0, \tag{9b}$$

$$EI_z V''(0) = 0, \quad V(0) = 0, \quad E\Gamma\theta''(0) = 0, \quad \theta(0) = 0, \tag{9c}$$

$$EI_z V'''(L) + M\omega^2(V(L) + V'(L)p + \theta(L)s) - k_L(V'(L)\bar{x} + \theta(L)\bar{z} + V(L)) = 0, \tag{9d}$$

$$\begin{aligned} &E\Gamma\theta'''(L) - GJ\theta'(L) + \omega^2(\hat{I}_{\bar{x}\bar{x}}\theta(L) + MsV(L) + V'(L)\hat{I}_{\bar{x}\bar{z}}) \\ &\quad - k_L(V'(L)\bar{z}\bar{x} + \theta(L)\bar{z}^2 + V(L)\bar{z}) - k_B\theta(L) = 0, \end{aligned} \tag{9e}$$

$$\begin{aligned} &EI_z V''(L) - \omega^2(V'(L)\hat{I}_{\bar{z}\bar{z}} + V(L)pM + \theta(L)\hat{I}_{\bar{x}\bar{z}}) \\ &\quad + k_L(V'(L)\bar{x}^2 + \theta(L)\bar{x}\bar{z} + V(L)\bar{x}) = 0, \end{aligned} \tag{9f}$$

$$\theta''(L) = 0 \quad \text{or} \quad \theta'(L) = 0, \tag{9g}$$

where primes denote derivatives with respect to spatial coordinate x. Implementing the same method presented in Ref. [14] to solve Eqs. (8a) and (8b), amplitude functions $V(x)$ and $\theta(x)$ can

be found as

$$V(x) = \hat{C}_1 \cos \alpha_1 x + \hat{C}_2 \sin \alpha_1 x + \hat{C}_3 \cos \alpha_2 x + \hat{C}_4 \sin \alpha_2 x + \hat{C}_5 \cosh \alpha_3 x + \hat{C}_6 \sinh \alpha_3 x + \hat{C}_7 \cosh \alpha_4 x + \hat{C}_8 \sinh \alpha_4 x, \tag{10}$$

$$\theta(x) = \beta_1(\hat{C}_1 \cos \alpha_1 x + \hat{C}_2 \sin \alpha_1 x) + \beta_2(\hat{C}_3 \cos \alpha_2 x + \hat{C}_4 \sin \alpha_2 x) + \beta_3(\hat{C}_5 \cosh \alpha_3 x + \hat{C}_6 \sinh \alpha_3 x) + \beta_4(\hat{C}_7 \cosh \alpha_4 x + \hat{C}_8 \sinh \alpha_4 x), \tag{11}$$

$$\beta_i = \frac{\lambda_B \alpha_i^4 - 1}{c} \ (i = 1, \ldots, 4), \ \alpha_1 = \sqrt{|\kappa_1|}, \ \alpha_2 = \sqrt{|\kappa_2|}, \ \alpha_3 = \sqrt{\kappa_3}, \ \alpha_4 = \sqrt{\kappa_4}, \tag{12}$$

where $\hat{C}_i$ $(i = 1, 2, \ldots, 8)$ are unknown amplitude coefficients to be determined from the boundary conditions, and λ_B is defined as $\lambda_B = EI_z/m\omega^2$. κ_i $(i = 1, 2, 3, 4)$ are the roots of the characteristic quartic polynomial of the ordinary differential equation obtained via reducing Eqs. (8a) and (8b) into one equation which contains merely $V(x)$ and its derivatives up to eight order. Bishop et al. [8] showed that this quartic equation has four real roots, two of them negative and two remaining positive. For a beam with clamped-attached tip mass end conditions, the use of Eqs. (9b) and (9d)–(9g) yields a set of eight linear homogeneous equations which can be written in matrix form

$$\hat{\mathbf{A}}\hat{\mathbf{C}} = \mathbf{0}, \tag{13}$$

where $\hat{\mathbf{A}}$ is an 8×8 nonsymmetric matrix while $\hat{\mathbf{C}}$ is a vector which contains $\hat{C}_i$ $(i = 1, 2, \ldots, 8)$ constants. Nontrivial solutions of Eq. (13) correspond to the ω values satisfying the following frequency equation

$$\det(\hat{\mathbf{A}}) = 0. \tag{14}$$

3. The orthogonality condition

The orthogonality condition associated with the modal functions is as follows:

$$\int_0^L [mV_iV_j + mc(\theta_iV_j + \theta_jV_i) + I_s\theta_i\theta_j]\,\mathrm{d}x + M[pV_i'(L)V_j(L) + V_i(L)V_j(L) + s\theta_i(L)V_j(L) + pV_i(L)V_j'(L) + sV_i(L)\theta_j(L)] + \hat{I}_{\bar{z}\bar{z}}V_i'(L)V_j'(L) + \hat{I}_{\bar{x}\bar{z}}\{\theta_i(L)V_j'(L) + \theta_j(L)V_i'(L)\} + \hat{I}_{\bar{x}\bar{x}}\theta_i(L)\theta_j(L) = \widehat{A}_{ij}, \tag{15}$$

where $\widehat{A}_{ij}$ is a real number defined as: $\widehat{A}_{ij} \neq 0$ if $i = j$; $\widehat{A}_{ij} = 0$ if $i \neq j$. Comparison of Eq. (15) with Eq. (30) in Ref. [5] reveals that the terms added to the integral are similar, while the integral in Eq. (15) differs from the one in Ref. [5], since the beams considered in these studies have different geometric properties.

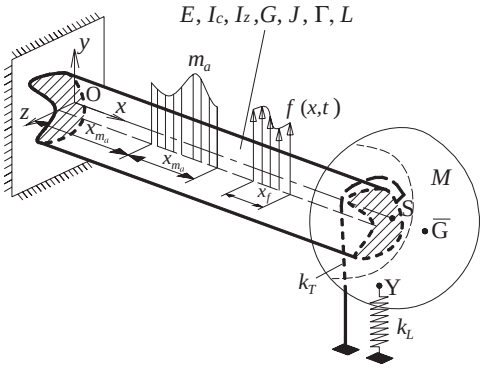

Fig. 4. The system with an additional attachment in-span.

4. Forced vibration analysis

Assume that the system in Fig. 1 has also a distributed mass in-span of m_a per unit length as shown in Fig. 4. Then, equations of motion for this case can be given as

$$EI_z w_{xxxx} + (m + m_a H_1(x, x_{m_a}, \Delta x_{m_a}))(\ddot{w} + c\ddot{\psi}) = H_2(x, x_f, \Delta x_f) f(x, t), \tag{16a}$$

$$E\Gamma\psi_{xxxx} - GJ\psi_{xx} + c(m + m_a H_1(x, x_{m_a}, \Delta x_{m_a}))(\ddot{w} + c\ddot{\psi}) + I_c\ddot{\psi} = cH_2(x, x_f, \Delta x_f) f(x, t), \tag{16b}$$

where H_i $(i = 1, 2)$ are Heaviside functions defined as follows:

$$H_1 = H(x - x_{m_a}) - H(x - (x_{m_a} + \Delta x_{m_a})), \tag{17a}$$

$$H_2 = H(x - x_f) - H(x - (x_f + \Delta x_f)). \tag{17b}$$

To apply Galerkin's discretization procedure, it is assumed that product solutions for Eq. (16) exist as follows:

$$w(x, t) = \sum_{i=1}^{n} V_i(x)\widehat{q}_i(t) = \mathbf{V}^{\mathrm{T}}\widehat{\mathbf{q}}, \quad \psi(x, t) = \sum_{i=1}^{n} \theta_i(x)\widehat{q}_i(t) = \boldsymbol{\theta}^{\mathrm{T}}\widehat{\mathbf{q}}, \tag{18}$$

where n denotes the number of modes included, $\widehat{\mathbf{q}}$, $\mathbf{V}$ and $\boldsymbol{\theta}$ are the column matrices of generalized coordinates, bending and torsional amplitude functions, respectively. Substituting Eq. (18) into Eqs. (16a) and (16b), multiplying Eq. (16a) by $\mathbf{V}$ and Eq. (16b) by $\boldsymbol{\theta}$, then adding the resulting equations yield

$$\mathbf{M}_T\ddot{\widehat{\mathbf{q}}} + \mathbf{K}_T\widehat{\mathbf{q}} = \mathbf{Q}. \tag{19}$$

$\mathbf{M}_T$, $\mathbf{K}_T$ and $\mathbf{Q}$ in Eq. (19) are the symmetric mass matrix, nonsymmetric stiffness matrix and column matrix of generalized forces, respectively. These matrices are defined as follows:

$$\mathbf{K}_T = \int_0^L (EI_z\mathbf{V}\mathbf{V}''''^{\mathrm{T}} + E\Gamma\boldsymbol{\theta}\boldsymbol{\theta}''''^{\mathrm{T}} - GJ\boldsymbol{\theta}\boldsymbol{\theta}''^{\mathrm{T}})\,\mathrm{d}x = (\mathrm{diag}(\omega^2\widehat{A}) - \mathrm{diag}(\omega^2)\tilde{\mathbf{M}})^{\mathrm{T}}, \tag{20}$$

$$\mathbf{M}_T = \int_0^L ((m + m_a H_1)(\mathbf{V}\mathbf{V}^{\mathrm{T}} + c\mathbf{V}\boldsymbol{\theta}^{\mathrm{T}} + c\boldsymbol{\theta}\mathbf{V}^{\mathrm{T}} + c^2\boldsymbol{\theta}\boldsymbol{\theta}^{\mathrm{T}}) + I_c\boldsymbol{\theta}\boldsymbol{\theta}^{\mathrm{T}})\,\mathrm{d}x, \tag{21}$$

$$\mathbf{Q} = \int_0^L H_2 f(x,t)(\mathbf{V} + c\boldsymbol{\theta})\,\mathrm{d}x, \tag{22}$$

$$\begin{aligned}\bar{\mathbf{M}} = [&M\mathbf{V}\mathbf{V}^{\mathrm{T}} + Mp(\mathbf{V}'\mathbf{V}^{\mathrm{T}} + \mathbf{V}\mathbf{V}'^{\mathrm{T}}) + Ms(\boldsymbol{\theta}\mathbf{V}^{\mathrm{T}} + \mathbf{V}\boldsymbol{\theta}^{\mathrm{T}}) + \hat{I}_{\bar{z}\bar{z}}\mathbf{V}'\mathbf{V}'^{\mathrm{T}} \\ &+ \hat{I}_{\bar{x}\bar{x}}\boldsymbol{\theta}\boldsymbol{\theta}^{\mathrm{T}} + \hat{I}_{\bar{x}\bar{z}}(\boldsymbol{\theta}\mathbf{V}'^{\mathrm{T}} + \mathbf{V}'\boldsymbol{\theta}^{\mathrm{T}})]_{x=L},\end{aligned} \tag{23}$$

where the orthogonality relation given by Eq. (15) is used to obtain Eq. (20). In the absence of external force $f(x,t)$, modal analysis of the system in Fig. 4 can be performed by solving the eigenvalue problem

$$(\mathbf{K}_T - \varpi^2\mathbf{M}_{\mathrm{T}})\hat{\mathbf{q}} = \mathbf{0}. \tag{24}$$

ϖ in Eq. (24) shows natural frequencies of the overall system with in-span attachment, and $\hat{\mathbf{q}}$ is the column vector of unknown amplitude coefficients.

5. Numerical results

5.1. Verification of the present model

In this section, firstly, some limiting cases are studied to verify the model presented here. To this end, two types of beams, i.e. the beam with semi-circular open cross section (SC), and the other one with channel cross section (CC) shown in Fig. 5, are considered. The physical properties of both beams are taken from Ref. [14], and for the completeness of the work they are also given in Table 2. Comparison of the numerical results by the current study with those given in Ref. [14] for different support types is presented in Table 3. Components of the inertia tensor about the center of tip mass are always taken as in Table 3 throughout the present paper.

To obtain clamped-free end conditions, all the attachments at the right end of the beam are ignored in the present model, and boundary conditions in Eq. (5b) are used for the left end. The

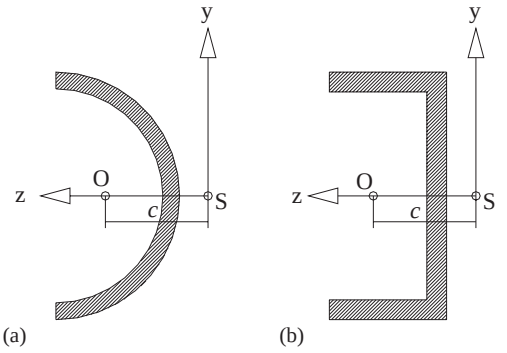

Fig. 5. Two types of beams considered in numerical calculations. (a) SC beam, (b) CC beam.

Table 2
Physical properties of the beams used in numerical calculations

	SC	CC
E	68.9×10^9 N/m^2	2.164×10^{11} N/m^2
G	26.5×10^9 N/m^2	0.801×10^{11} N/m^2
I_z	9.26×10^{-8} m^4	0.45×10^{-6} m^4
I_s	0.000501 kg m	0.00725 kg m
J	1.64×10^{-9} m^4	0.14×10^{-9} m^4
Γ	1.52×10^{-12} m^6	0.1636×10^{-9} m^6
L	0.82 m	1.28 m
m	0.835 kg/m	2.095 kg/m
c	0.0155 m	0.03771 m

SC: Beam with semi-circular cross section, CC: beam with channel cross section.

Table 3
Comparison of the natural frequencies (Hz) obtained by the present model with those from Ref. [14]

Support type	Clamped–free				Clamped–clamped				Simple–simple			
Beam type	SC		CC		SC		CC		SC		CC	
Modal index	I$^{(*)}$	II	I$^{(*)}$	II	I$^{(**)}$	II	I$^{(**)}$	II	I$^{(***)}$	II	I$^{(***)}$	II
1	63.79	63.79	25.37	25.37	198.81	198.81	149.40	149.40	150.44	150.44	67.13	67.12
2	137.68	137.68	98.56	98.55	425.05	425.04	410.58	410.58	320.32	320.32	263.66	263.67
3	278.36	278.35	148.65	148.65	618.09	618.09	624.54	624.53	365.81	365.81	275.76	275.75
4	484.77	484.77	411.57	411.57	695.64	695.63	803.85	803.84	604.13	604.13	591.13	591.23
5	663.78	663.84	615.39	615.39	999.32	999.31	1327.99	1327.99	885.01	885.01	1049.49	1049.80

I: Present study, II: reference work [14]. Coordinates of the tip mass gravitational center $\bar{G}$ are chosen as: $p = c,\ q = 0.25c,\ s = 1.25c$. The components of the inertia tensor about center of gravity are: $I_{\bar{x}\bar{x}} = 5.428.10^{-4}M/(mL),\ I_{\bar{z}\bar{z}} = 4.711.10^{-4}M/(mL), I_{\bar{x}\bar{z}} = -2.729.10^{-6}M/(mL)$. Points Y and S in Fig. 1 are coincident so long as linear spring of stiffness k_L is present.

$^{(*)}$: $k_L = k_T = 0, M = 0, m_a = 0$.

$^{(**)}$: $M = 10^8(mL),\ k_L = k_T = 0,\ m_a = 0$.

$^{(***)}$: $k_L = 10^6 EI_z/L^3,\ k_T = 10^6 GJ/L,\ M = 0,\ m_a = 0$.

resulting frequencies for this supporting type are in very good agreement with the ones from Ref. [14] as seen from Table 3. Although the dynamic transfer matrix method is used in Ref. [14], the results obtained are exact since analytical solutions of the equations of motion are used to set the transfer matrix.

Ignoring all attachments but tip mass, and increasing the tip mass M largely leads to a beam with clamped end condition at the limit, which may not have practical importance. On the other hand, supporting the right end of the beam in Fig. 1 with linear and torsional springs of high

stiffness, and omitting the tip mass gives the simply supported end condition at the limit. Comparison of the frequencies obtained in this model for different end conditions with those conveyed by the earlier work reveals that the present model is useful and generative.

5.2. Effect of tip mass on frequencies and modal shapes

To examine the effect of tip mass on natural frequencies and modal shapes of the beams shown in Fig. 5, various values within the interval $\{0, 10(mL)\}$ for the tip mass are considered, and the corresponding frequencies are presented in Table 4, where the columns entitled "$\%d$" denote the decrease in frequencies in percentage. For instance; $\%d = -85 = ((9.77 - 63.79)/63.79) \times 100$. The normalized modal shape functions of both beams are illustrated in Figs. 6 and 7, respectively. The modal functions are normalized in a similar way in Ref. [9], where torsional amplitude function $\theta(x)$ is multiplied by the shear center offset c so as to compare directly with $V(x)$ and understand which function is dominant in the overall shape of the mode considered.

With increasing tip mass, a decrease in natural frequencies is observed as expected. Furthermore, the second frequencies of both beams fall sharply. Considering Rayleigh's quotient, the reason why the second natural frequency is affected the most by the change in tip mass amount can be explained as follows: Vibration amplitudes and modal shapes corresponding to the first two modes are nearly the same for each beam as seen from Figs. 6 and 7. This means that maximum potential energies of both modes are of nearly the same order, while the reference kinetic energy of the second mode is greater than that of the first mode. Consequently, the second natural frequencies for both beams are much more affected by the variation of tip mass amount. As the modal index rises, the effect of tip mass on the frequencies weakens since motion amplitudes become smaller with increasing frequency, which corresponds to an insignificant change in reference kinetic energy. Because the right end of the beam loses its ability of motion, one can conclude from Figs. 6 and 7 that modal shapes are more affected by the increase in tip mass especially in the higher modes.

Table 4
Effect of tip mass on natural frequencies of the system without distributed mass for two different beams (SC and CC)

Modal index	SC					CC				
	I	II	III	IV	$\%d$	I	II	III	IV	$\%d$
1	63.79	53.96	28.21	9.77	−85	25.37	32.66	19.17	6.93	−72
2	137.68	107.34	48.73	16.23	−88	98.56	85.70	47.21	17.00	−82
3	278.36	236.19	196.15	184.30	−33	148.65	186.24	157.58	146.04	−1.7
4	484.77	442.79	394.48	306.39	−36	411.57	437.71	379.72	313.92	−24
5	663.84	548.26	470.61	435.89	−34	615.39	555.33	468.66	426.12	−30

I: $M = 0$, II: $M = 0.1(mL)$, III: $M = (mL)$, IV: $M = 10(mL)$.
Left ends ($x = 0$) are clamped for both beams.
$\%d$: decrease percentage between I and IV.
Coordinates of point $\tilde{G}$ in Fig. 1 are: $p = q = s = c$.

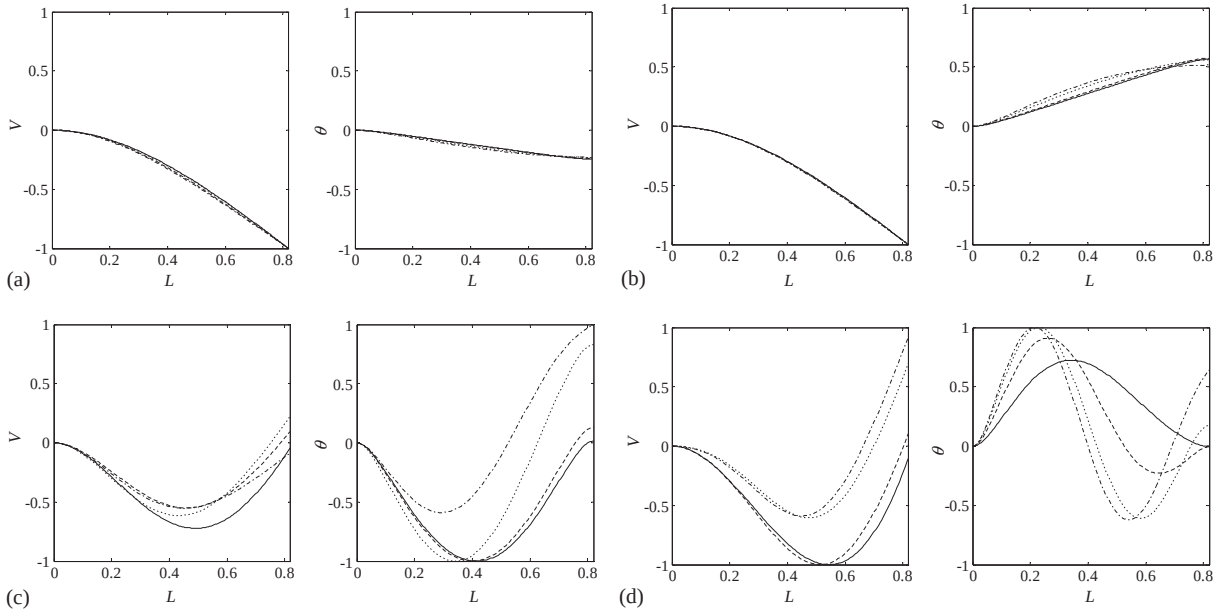

Fig. 6. Effect of tip mass on modal shapes of cantilever beam with SC. (a) First mode, (b) second mode, (c) third mode, (d) fourth mode, $V : V(x)$, $\theta : \theta(x)$. ------: $M = 0$, ----------: $M = 0.1(mL)$, ----: $M = (mL)$, ——: $M = 10(mL)$. $m_a = 0$, $p = q = s = c$.

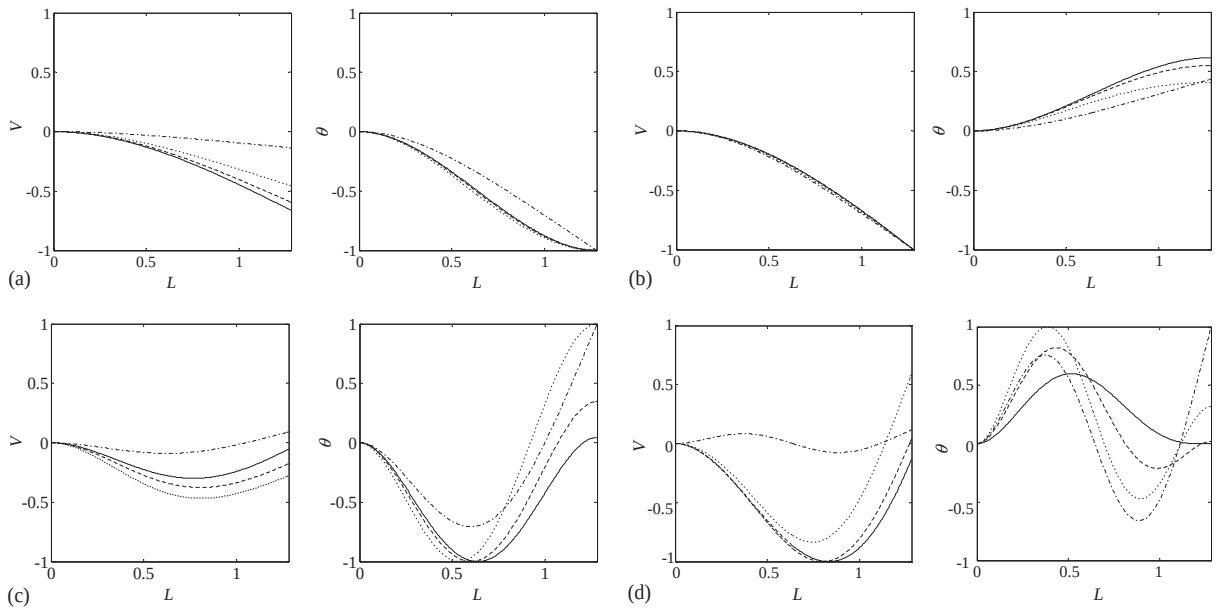

Fig. 7. Effect of tip mass on modal shapes of the cantilever beam with CC. (a) First mode, (b) second mode, (c) third mode, (d) fourth mode, $V : V(x)$, $\theta : \theta(x)$. ------: $M = 0$, ----------: $M = 0.1(mL)$, ----: $M = (mL)$, ——: $M = 10(mL)$. $m_a = 0$, $p = q = s = c$.

5.3. Effect of distributed mass on frequencies and modal shapes

To investigate the effect of distributed mass on modal shapes and natural frequencies, cantilever beam with CC will be considered again. In Case 1, the variation of natural frequencies for various amounts of the distributed mass m_a whose beginning point x_{m_a} and distribution length Δx_{m_a} are fixed is studied. On the other hand, how the natural frequencies and modal shapes are affected by the distributed mass of constant m_a and Δx_{m_a} but variable x_{m_a} is treated in Case 2. Numerical results for Cases 1 and 2 are presented in Tables 5 and 6, while the associated modal shapes are illustrated in Figs. 8 and 9, respectively. Eight term modal expansions of the clamped-free beam are used for both bending and torsion to carry out numerical calculations.

As expected, the frequencies decrease with increasing distributed mass amount, see Table 5. Although monotone falling in the first frequency should be expected as the distributed mass location is shifted to the free end of the beam (since the first mode is bending dominant and does not have a nodal point), the first frequency value in the rightmost column of Table 6 seems to be contrary to this expectation. However, as is seen from Table 6, the distribution length of the distributed mass is $\Delta x_{m_a} = 0.05L$ m for the last location, while the first four are of $\Delta x_{m_a} = 0.1L$ m. A possible reason is that the distributed mass contributes to the total kinetic energy of the system less than the previous location when it is located at $x_{m_a} = 0.95L$. On the other hand, as bending deformation of the beam is also dominant in the second mode (see Fig. 9b), and the contribution

Table 5
Effect of distributed mass with fixed location on the first five natural frequencies (Hz) of the cantilever beam with CC (Case 1)

Modal index	$m_a = 0$	$m_a = 2m$	$m_a = 5m$	$m_a = 10m$
1	25.37	23.14	20.63	17.77
2	98.56	90.57	84.42	79.58
3	148.65	148.16	147.52	146.53
4	411.57	402.38	394.44	386.34
5	615.39	612.91	609.72	605.15

$x_{m_a} = 0.75L$, $\Delta x_{m_a} = 0.1L$.

Table 6
Effect of distributed mass with varying location on the first five natural frequencies (Hz) of the cantilever beam with CC (Case 2)

Modal index	$x_{m_a} = 0$	$x_{m_a} = 0.3L$	$x_{m_a} = 0.5L$	$x_{m_a} = 0.8L$	$x_{m_a} = 0.9L$
1	25.37	24.54	22.05	16.94	18.33
2	98.55	93.09	84.64	78.94	77.82
3	148.39	117.43	125.52	144.41	136.47
4	407.01	332.47	392.56	397.45	374.82
5	614.05	552.74	516.10	592.76	563.34

$\Delta x_{m_a} = 0.05L$ for $x_{m_a} = 0.9L$, otherwise $\Delta x_{m_a} = 0.1L$, $m_a = 10m$ for all x_{m_a} values.

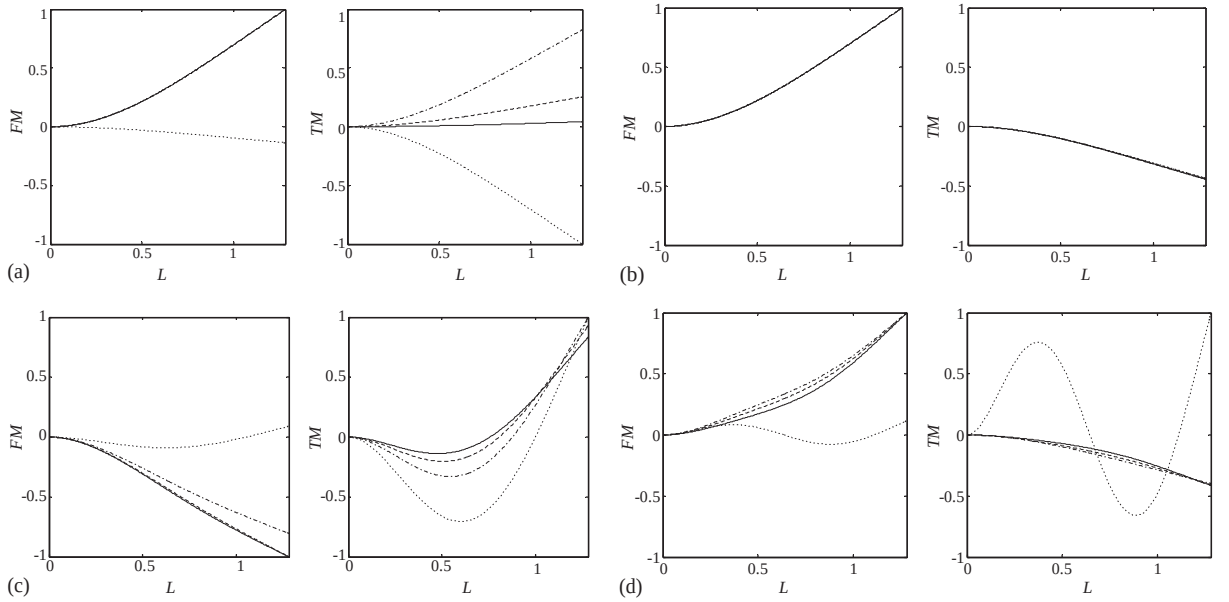

Fig. 8. Effect of distributed mass with fixed location on modal shapes of the cantilever beam with CC. --------: $m_a = 0$, – – – – –: $m_a = 2m$, – – – –: $m_a = 5m$, ——: $m_a = 10m$. $x_{m_a} = 0.75L$, $\Delta x_{m_a} = 0.1L$. FM: flexural mode ($\sum_{i=1}^{8} V_i \hat{q}_i, \hat{q}_i$: modal coefficients), TM: torsional mode $\left(\sum_{i=1}^{8} \theta_i \hat{q}_i\right)$.

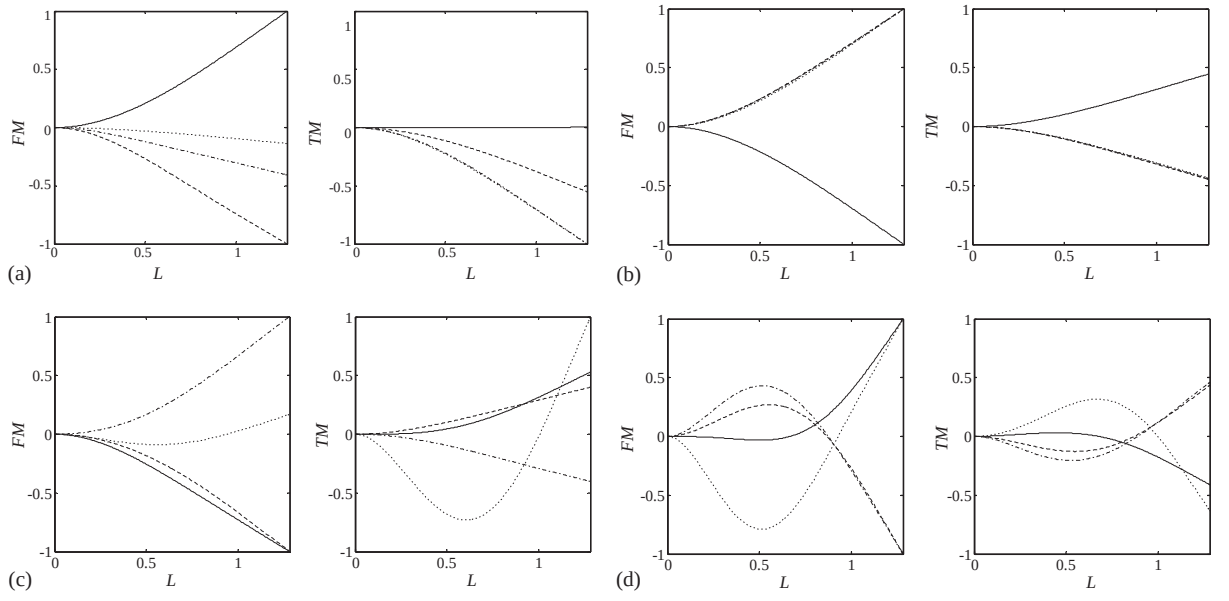

Fig. 9. Effect of distributed mass with varying location on modal shapes of the cantilever beam with CC. --------: $x_{m_a} = 0$, – – – – –: $x_{m_a} = 0.3L$, – – – –: $x_{m_a} = 0.5L$, ——: $x_{m_a} = 0.8L$. $\Delta x_{m_a} = 0.1L$, $m_a = 10m$. TM: torsional mode $\left(\sum_{i=1}^{8} \theta_i \hat{q}_i\right)$, FM: flexural mode $\left(\sum_{i=1}^{8} V_i \hat{q}_i\right)$.

of the distributed mass to the total kinetic energy is more in the second mode than in the first mode while the change in maximum potential energy is small enough to neglect, a continuous decrease in the frequency indicates a reasonable variation. Bending and torsion equally contribute to the formation of the related mode as the modal index rises. Moreover, nodal points begin to appear. Hence, it is conceivable that there occur fluctuations in frequencies of the upper modes (see Table 6) as the distributed mass location is shifted to the right end of the beam. The second mode of the CC beam appears to be less affected by the variations of both x_{m_a} and m_a, as seen from Figs. 8b and 9b. Note that the fifth column for $x_{m_a} = 0.9L$ is added to draw attention to the interesting variation in the first frequency. Therefore, modal shape curves corresponding to this value of x_{m_a} are not plotted.

Ignoring all the attachments except for the distributed mass and tip mass, deflection of terminal point of the centroidal axis of the beam with CC is shown in Fig. 10 for four different distributed

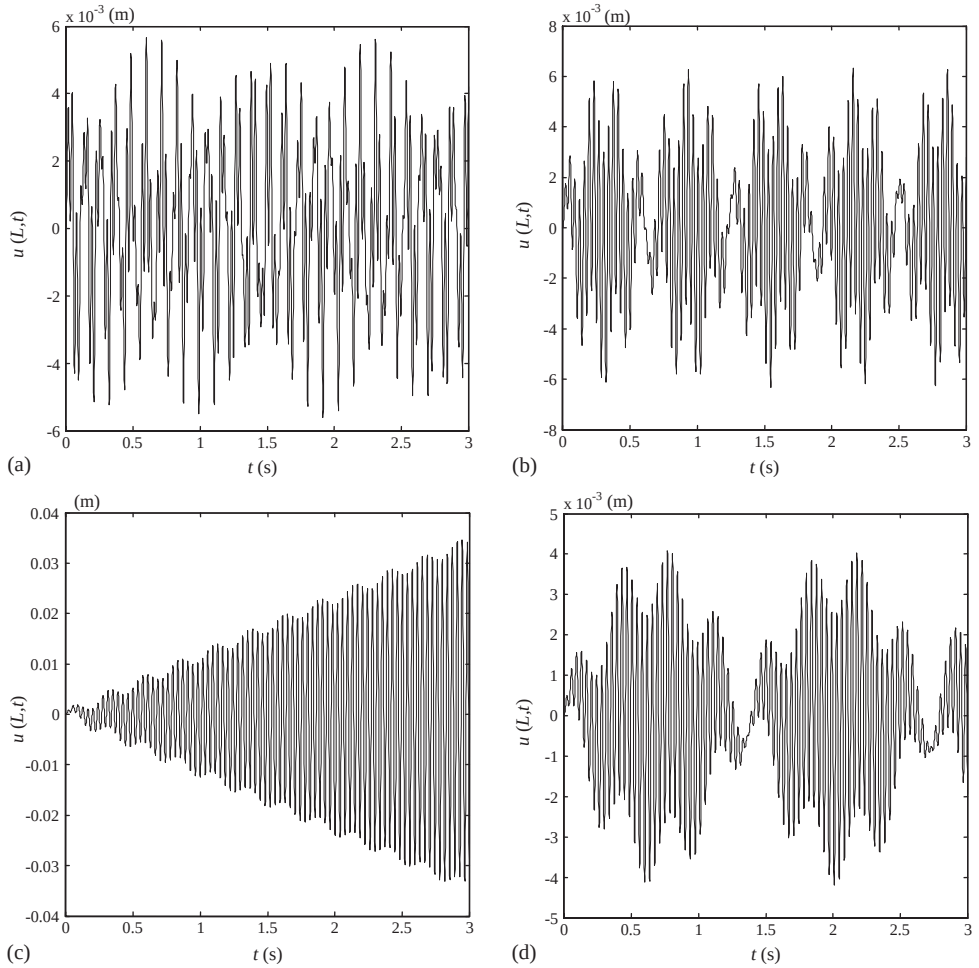

Fig. 10. Time-varying deflection of tip point of the centroidal axis of the beam with CC for various distributed mass amounts. (a) $m_a = 0$, (b) $m_a = 10m$, (c) $m_a = 30m$, (d) $m_a = 60m$. $M = 2(mL)$, $p = 0$, $q = -2c$, $s = 2c$, $k_L = 0$, $k_T = 0$. $x_{m_a} = 0.9L$, $\Delta x_{m_a} = 0.05L$.

Table 7
Variation of the first four natural frequencies of the cantilever beam with CC

Modal index	$m_a = 0$	$m_a = 10m$	$m_a = 30m$	$m_a = 60m$
1	8.76	5.68	3.85	2.85
2	34.58	28.59	26.97	26.26
3	147.35	147.77	147.43	146.58
4	344.22	309.46	271.79	236.95

$\Delta x_{m_a} = 0.1L,\ M = 2(mL),\ p = 0,\ q = -2c,\ s = 2c,\ k_L = 0, k_T = 0.$

mass amounts, while the left end of the beam is clamped. The distributed force $f(x,t) = 100\ \sin(\omega_f t)\,\mathrm{N/m}$ with driving frequency $\omega_f = (27)2\pi\,\mathrm{rad/s}$ is applied in the span $\{x_f, (x_f + \Delta x_f)\}$, where $x_f = 0.9L$ and $\Delta x_f = 0.1L$. Since the point is on the centroidal axis, its displacement $u(L,t)$ along the y-axis is obtained by the following relation: $u(L,t) = w(L,t) + c\psi(L,t)$. This example is also an application of the orthogonality relation given by Eq. (17). The variation of the first four natural frequencies of the system as the distributed mass amount is increased is presented in Table 7. Since the second natural frequency is almost equal to the driving frequency of the force $f(x,t)$ when the distributed mass amount is $m_a = 30m$, tip point deflection shows a tendency to increase relatively as seen from Fig. 10c, i.e. nearly resonance is encountered. On the other hand, as the difference between the second frequency of the system and the driving frequency increases, the form of the displacement curve begins to resemble the mathematical form of the driving force as shown in Fig. 10a.

6. Conclusions

An exact analytical procedure is developed to obtain natural frequencies and mode shapes of a system consisting of a beam with monosymmetric open cross section carrying a tip mass of non-negligible dimensions and springs at one end. The model is verified by comparing the frequencies corresponding to the limiting cases of the present model with the ones from a previously published work. The orthogonality condition of amplitude functions is also derived and used for the forced vibration analysis of a channel cross section beam carrying a distributed mass in addition to the tip mass. Furthermore, the effects of tip mass and distributed mass on natural frequencies and modal shapes are investigated for two beams with different open cross sections. The frequencies numerically obtained for various attachment properties are tabulated, and the modal shape functions are plotted. Two significant conclusions drawn from the numerical applications are as follows:

(1) The second natural frequencies of both CC and SC beams fall noticeably with the increase in tip mass amount.
(2) The second mode of the CC beam is affected the least by the change in both the distributed mass amount m_a and its location x_{m_a}.

Appendix A. Derivation of the equations of motions

With the help of the illustration in Fig. 3, the relations among coordinate frames can be obtained as in the following:

$$\hat{\mathbf{b}} = \mathbf{T}_1\hat{\mathbf{a}}, \quad \mathbf{T}_1 = \begin{bmatrix} \cos\alpha & \sin\alpha & 0 \\ -\sin\alpha & \cos\alpha & 0 \\ 0 & 0 & 1 \end{bmatrix}, \quad \alpha = w_x(L,t), \tag{A.1}$$

$$\hat{\mathbf{c}} = \mathbf{T}_2\hat{\mathbf{b}}, \quad \mathbf{T}_2 = \begin{bmatrix} 1 & 0 & 0 \\ 0 & \cos\beta & -\sin\beta \\ 0 & \sin\beta & \cos\beta \end{bmatrix}, \quad \beta = \psi(L,t), \tag{A.2}$$

$$\hat{\mathbf{c}} = \mathbf{T}_3\hat{\mathbf{a}}, \quad \mathbf{T}_3 = \mathbf{T}_2\mathbf{T}_1 \tag{A.3}$$

where $\hat{\mathbf{a}}, \hat{\mathbf{b}}$ and $\hat{\mathbf{c}}$ are column matrices with the elements $\mathbf{a}_i, \mathbf{b}_i$ and $\mathbf{c}_i$ $(i = 1, 2, 3)$, respectively. $\mathbf{T}_1$, $\mathbf{T}_2$ and $\mathbf{T}_3$ are transformation matrices relating unit vectors of different coordinate frames with each other. Assuming small-angle approach, $\mathbf{T}_3$ can be written as

$$\mathbf{T}_3 = \begin{bmatrix} 1 & \alpha & 0 \\ -\alpha & 1 & -\beta \\ 0 & \beta & 1 \end{bmatrix}. \tag{A.4}$$

The position vector of a differential beam element $\mathbf{r}_P$ and the displacement vector of the point Y can be given directly by using the above definitions as

$$\begin{aligned} \mathbf{r}_P = {} & (L + p + \bar{p} - (q + \bar{q})\alpha)\mathbf{a}_1 + (w_L + \alpha(p + \bar{p}) + \beta(s + \bar{s}) + q + \bar{q})\mathbf{a}_2 \\ & + (s + \bar{s} - (q + \bar{q})\beta)\mathbf{a}_3, \end{aligned} \tag{A.5}$$

$$\mathbf{OY} = (\bar{x} - \bar{y}\alpha + L)\mathbf{a}_1 + (\bar{x}\alpha + \bar{y} + \bar{z}\beta + w_L)\mathbf{a}_2 + (-\bar{y}\beta + \bar{z})\mathbf{a}_3. \tag{A.6}$$

As stated earlier, the y component of the vector in Eq. (A.6) is considered to describe the deformation in the linear spring of stiffness k_L. Therefore,

$$\Delta\mathbf{Y} = [[\mathbf{OY}(t) - \mathbf{OY}(0)]\mathbf{a}_2]\mathbf{a}_2 = (\alpha\bar{x} + \beta\bar{z} + w_L)\mathbf{a}_2. \tag{A.7}$$

Now, variations of the terms in Eqs. (1) and (2) can be given as follows:

$$\frac{1}{2}\int_{t_1}^{t_2} \delta\left(\int_0^L m(\dot{w} + c\dot{\psi})^2 \,\mathrm{d}x\right)\mathrm{d}t = -\int_{t_1}^{t_2}\int_0^L (m(\ddot{w} + c\ddot{\psi})\delta w + mc(\ddot{w} + c\ddot{\psi})\delta\psi)\,\mathrm{d}x\,\mathrm{d}t, \tag{A.8}$$

$$\frac{1}{2}\int_{t_1}^{t_2} \delta\left(\int_0^L I_c\dot{\psi}^2 \,\mathrm{d}x\right)\mathrm{d}t = -\int_{t_1}^{t_2}\int_0^L I_c\ddot{\psi}\delta\psi \,\mathrm{d}x\,\mathrm{d}t, \tag{A.9}$$

$$\frac{1}{2}\int_{t_1}^{t_2}\delta\left(\int_{\bar{B}}(\dot{\mathbf{r}}_P)^2\,\mathrm{d}M\right)\mathrm{d}t = -\int_{t_1}^{t_2}\delta w_x(L,t)\left\{\ddot{w}_x(L,t)\hat{I}_{\bar{z}\bar{z}}+\ddot{w}_L pM+\ddot{\psi}_L\hat{I}_{\bar{x}\bar{z}}\right\}\mathrm{d}t$$
$$-\int_{t_1}^{t_2}\delta\psi_L\{\ddot{w}_x(L,t)\hat{I}_{\bar{x}\bar{z}}+\ddot{w}_L sM+\ddot{\psi}_L\hat{I}_{\bar{x}\bar{x}}\}\,\mathrm{d}t$$
$$-\int_{t_1}^{t_2}\delta w_L\{\ddot{w}_L M+(\ddot{w}_x(L,t)p+\ddot{\psi}_L s)M\}\,\mathrm{d}t, \tag{A.10}$$

$$\frac{1}{2}\int_{t_1}^{t_2}\delta\left(\int_0^L EI_z(w_{xx}^2)\,\mathrm{d}x\right)\mathrm{d}t=\int_{t_1}^{t_2}\left[EI_z w_{xx}\delta w_x|_0^L-EI_z w_{xxx}\delta w|_0^L+\int_0^L EI_z w_{xxxx}\delta w\,\mathrm{d}x\right]\mathrm{d}t, \tag{A.11}$$

$$\frac{1}{2}\int_{t_1}^{t_2}\delta\left(\int_0^L GJ(\psi_x^2)\,\mathrm{d}x\right)\mathrm{d}t=\int_{t_1}^{t_2}\left[GJ\psi_x\delta\psi|_0^L-\int_0^L GJ\psi_{xx}\delta\psi\,\mathrm{d}x\right]\mathrm{d}t, \tag{A.12}$$

$$\frac{1}{2}\int_{t_1}^{t_2}\delta\left(\int_0^L E\Gamma(\psi_{xx}^2)\,\mathrm{d}x\right)\mathrm{d}t=\int_{t_1}^{t_2}\left[E\Gamma\psi_{xx}\delta\psi_x|_0^L-E\Gamma\psi_{xxx}\delta\psi|_0^L+\int_0^L E\Gamma\psi_{xxxx}\delta\psi\,\mathrm{d}x\right]\mathrm{d}t, \tag{A.13}$$

$$\frac{1}{2}\int_{t_1}^{t_2}\delta(k_L(\Delta\mathbf{Y})^2)\,\mathrm{d}t=k_L\int_{t_1}^{t_2}\delta w_x(L,t)\{\bar{x}^2w_x(L,t)+\bar{x}\bar{z}\psi_L+\bar{x}w_L\}\,\mathrm{d}t$$
$$+k_L\int_{t_1}^{t_2}\delta\psi_L\{\bar{x}\bar{z}w_x(L,t)+\bar{z}^2\psi_L+\bar{z}w_L\}\,\mathrm{d}t$$
$$+k_L\int_{t_1}^{t_2}\delta w_L\{\bar{x}w_x(L,t)+\bar{z}\psi_L+w_L\}\,\mathrm{d}t, \tag{A.14}$$

$$\frac{1}{2}\int_{t_1}^{t_2}\delta(k_B(\psi_L)^2)\,\mathrm{d}t=\int_{t_1}^{t_2}k_B\psi_L\delta\psi_L\,\mathrm{d}t. \tag{A.15}$$

Employing Eqs. (A.8)–(A.15) in the Hamilton's integral leads to

$$\delta\int_{t_1}^{t_2}(T-U)\,\mathrm{d}t=\int_{t_1}^{t_2}\Big[-m\int_0^L(\ddot{w}+c\ddot{\psi})\delta w\,\mathrm{d}x-mc\int_0^L(\ddot{w}+c\ddot{\psi})\delta\psi\,\mathrm{d}x-I_c\int_0^L\ddot{\psi}\delta\psi\,\mathrm{d}x$$
$$-\delta w_x(L,t)\{\ddot{w}_x(L,t)\hat{I}_{\bar{z}\bar{z}}+\ddot{w}_L pM+\ddot{\psi}_L\hat{I}_{\bar{x}\bar{z}}\}-\delta\psi_L\{\ddot{w}_x(L,t)\hat{I}_{\bar{x}\bar{z}}+\ddot{w}_L sM+\ddot{\psi}_L\hat{I}_{\bar{x}\bar{x}}\}$$
$$-\delta w_L M\{\ddot{w}_L+\ddot{w}_x(L,t)p+\ddot{\psi}_L s\}-EI_z w_{xx}\delta w_x|_0^L+EI_z w_{xxx}\delta w|_0^L$$
$$-\int_0^L EI_z w_{xxxx}\delta w\,\mathrm{d}x-GJ\psi_x\delta\psi|_0^L+\int_0^L GJ\psi_{xx}\delta\psi\,\mathrm{d}x-E\Gamma\psi_{xx}\delta\psi_x|_0^L$$

$$+ E\Gamma\psi_{xxx}\delta\psi|_0^L - \int_0^L E\Gamma\psi_{xxxx}\delta\psi\,\mathrm{d}x - \delta w_x(L,t)k_L\{\bar{x}^2 w_x(L,t) + \bar{x}\bar{z}\psi_L + \bar{x}w_L\}$$
$$- k_L\delta\psi_L\{\bar{x}\bar{z}w_x(L,t) + \bar{z}^2\psi_L + \bar{z}w_L\} - k_L\delta w_L\{\bar{x}w_x(L,t) + \bar{z}\psi_L + w_L\}$$
$$- k_B\psi_L\delta\psi_L\Big]\,\mathrm{d}t = 0.$$

Grouping the terms with the same variational coefficients results in Eqs. (4) and (5).

References

[1] H. Abromovich, O. Hamburger, Vibration of a uniform cantilever Timoshenko beam with translational and rotational springs and with a tip mass, *Journal of Sound and Vibration* 154 (1) (1992) 67–80.

[2] M. Gürgöze, On the eigenfrequencies of a cantilever beam with attached tip mass and a spring–mass system, *Journal of Sound and Vibration* 190 (2) (1996) 149–162.

[3] K.T. Chan, X.Q. Wang, T.P. Leung, Free vibration of beams with two sections of distributed mass, *Journal of Vibration and Acoustics* 120 (1998) 944–948.

[4] J.S. Wu, H.M. Chou, Free vibration analysis of a cantilever beam carrying any number of elastically mounted point masses with the analytical-and-numerical-combined method, *Journal of Sound and Vibration* 213 (2) (1998) 317–332.

[5] D.C.D. Oguamanam, Free vibration of beams with finite mass rigid tip load and flexural–torsional coupling, *International Journal of Mechanical Sciences* 45 (2003) 963–979.

[6] S. Timoshenko, D.H. Young, W.J.R. Weaver, *Vibration Problems in Engineering*, Wiley, New York, 1974.

[7] E. Dokumaci, An exact solution for coupled bending and torsion vibrations of uniform beam having single cross-sectional symmetry, *Journal of Sound and Vibration* 119 (3) (1987) 443–449.

[8] R.E.D. Bishop, S.M. Cannon, S. Miao, On coupled bending and torsional vibration of uniform beams, *Journal of Sound and Vibration* 131 (1989) 457–464.

[9] A.N. Bercin, M. Tanaka, Coupled flexural–torsional vibrations of Timoshenko beams, *Journal of Sound and Vibration* 207 (1) (1997) 47–59.

[10] J.R. Banerjee, Explicit frequency equation and mode shapes of a cantilever beam coupled in bending and torsion, *Journal of Sound and Vibration* 224 (2) (1999) 267–281.

[11] C. Adam, Forced vibrations of elastic-bending torsion coupled beams, *Journal of Sound and Vibration* 221 (2) (1999) 273–287.

[12] S.H.R. Eslimy-Isfahany, J.R. Banerjee, Use of generalized mass in the interpretation of dynamic response of bending-torsion coupled beams, *Journal of Sound and Vibration* 238 (2) (2000) 295–308.

[13] S.M. Hashemi, M.J. Richard, Free vibrational analysis of axially loaded bending-torsion coupled beams: a dynamic finite element, *Computers and Structures* 77 (2000) 711–724.

[14] L. Jun, S. Rongying, H. Hongxing, J. Xianding, Coupled bending and torsional vibration of axially loaded Bernoulli–Euler beams including warping effects, *Applied Acoustics* 65 (2004) 153–170.